JOURNAL OF AIRCRAFT
Vol. 41, No. 4, July–August 2004

Time-Domain System Identification Methods for Aeromechanical and Aircraft Structural Modeling

Raman K. Mehra* and Ravi K. Prasanth†
Scientific Systems Company, Woburn, Massachusetts 01801

Time-domain model structures and algorithms are described that are suitable for the identification of aeromechanical and aircraft structural models from input–output data. An efficient batch subspace identification algorithm and its online version are presented. The batch algorithm was implemented and evaluated for structural mode identification of the V-22 tilt rotor and for the identification of models of aeromechanical instability. The online algorithm is demonstrated with a numerical example in which structural modes are identified and tracked as they appear. Our results and comparisons with current aircraft industry practice show several advantages of time-domain subspace methods over Prony and frequency-domain methods. Specific advantages include the ability to identify multiple structural modes simultaneously from a single experiment, the ability to use online system identification, and the ability to identify open-loop systems from closed-loop experimental data. These advantages have a significant effect on the number of ground and flight tests required and on how to perform testing in unstable flight regimes.

I. Introduction

A MODEL is a useful representation (or compression) of system dynamics. The precise meaning of useful is given by the application for which the model is intended. As a general rule, useful models of engineering systems must be computationally efficient. Another important requirement is the ability to describe system behaviors accurately under different extrapolated conditions, that is, the predictive power of the model. These two requirements are competing interests in that models that predict many system behaviors tend to be computationally hard and vice versa. For instance, Navier–Stokes equations have a lot more predictive power than the models discussed in this paper, but they are also numerically much harder. The modeler's task is to develop models that balance computational and predictive requirements, possibly by neglecting fine-scale structure and considering only those features that are dominant in the application. This is, of course, easier said than done in most flight dynamics problems, where distributed and nonlinear phenomena interact to produce complex dynamic behaviors. A good example is aircraft tail buffeting at high angles of attack, in which vortices shed from the wing impinge on the tail surface causing structural vibrations and eventually fatigue. Identification of models from experimental data appears to be the only avenue to solve such problems at the current time. Even in simpler settings, identification of model parameters such as stability derivatives is a requirement.

The system identification (SI) process shown in Fig. 1 is an iterative process consisting of experiment design, model structure determination, parameter estimation, and model validation.[1–3] Experiment design is concerned with the selection of test inputs and measurement variables, their sampling and conditioning, and other aspects that are directly related to the notion of an informative experiment. An experiment is said to be informative with respect to a model set if the experimental data allow discrimination between models in the set. Model structure selection and parameter estimation are simultaneous tasks, although, in practice, they are performed sequentially with model structure being selected first. The structure of a model is defined in terms of its nature, for example, linear, Wiener, neural network, order (number of free variables), and parameterization, for example, state space in modal coordinates. There are several considerations that go into model structure selection, including a priori knowledge, flexibility, and algorithmic complexity. After selecting a model structure, parameters of the model are estimated from experimental data. Minimum mean square estimation (MMSE) and maximum likelihood estimation (MLE) are the most common methods of parameter estimation.[1,2,4] Numerical procedures for estimation range from least squares to the expectation-maximization algorithm.[1,2,5] The final step of model validation is to determine the "goodness" of an identified model, that is, the extent to which it is useful in its intended application. Thus, a model identified for controller design may be deemed valid if the resulting controller produces satisfactory performance. When model validation fails, it may be due to the choice of model structure and the lack of information in experimental data. As shown in Fig. 1, the steps are iterated until a validated model is found. Details of these steps and the iterative process may be found in Refs. 1–4 and 6.

SI is by now widely recognized as an important tool in flight vehicle modeling, control, and data analysis. Hamel and Jategaonkar[7,8] give a detailed survey of literature, methods, and processes used in aircraft industry. Klein and Morelli[9] focus on aircraft aerodynamic modeling and provide easy-to-use software. There has also been tremendous amount of research in SI for rotorcraft modeling and control.[10–12] The ultimate aim of SI in many applications, including that of the present paper, is to determine a state-space or transfer function model that can be used for controller design. However, the aerodynamic stability derivatives and structural modes are functions of gross weight, airspeed, and many other factors, so that a large number of experiments will need to be performed to identify models suitable for controller design. We are, therefore, interested in developing and validating methods that are not restricted by the type of input used for identification[7,9,13] and that are capable of identifying multiple modes simultaneously. In advanced applications, there is a need to estimate and track structural modes online because they change slowly due to in-flight mass and inertia changes and abruptly due to battle damage. Online system identification is an integral part of many proposed vehicle health monitoring and control reconfiguration systems. Thus, SI methods that can rapidly and reliably estimate models in-flight are of interest. Another problem that arises in flight envelope expansion is the development of aircraft models at unstable flight conditions. It is known that active control of unstable aeromechanical phenomena such as ground and air resonance can expand the operational flight envelope of tilt rotors. However, there

Received 5 July 2003; revision received 23 September 2003; accepted for publication 24 September 2003.

*President, 500 West Cummings Park, Suite 3000; rkm@ssci.com. Member AIAA.

†Principal Research Scientist, 500 West Cummings Park; prasanth@ssci.com.

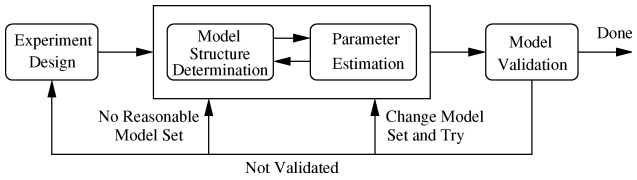

Fig. 1 Steps in SI.

is a severe lack of models for controller design because open-loop flight testing is not feasible.

This paper describes a class of time-domain SI methods suitable for aircraft aeromechanical and structural modeling. Section II and Appendices A and B present model structures and subspace identification algorithms for MMSE. Appendix A describes the standard subspace method for batch processing of multi-input/multi-output (MIMO) data. A recursive version of the standard algorithm is given in Appendix B. This online algorithm is capable of tracking structural modes in real-time as demonstrated by the numerical example in Sec. II. The batch version of subspace identification algorithm is demonstrated in Sec. III using structural mode identification of a V-22 tilt rotor. A comparison with the traditional Prony method is also provided. Section IV presents identification of models of aeromechanical instability using the batch algorithm. This application requires closed-loop experimentation and exemplifies the use of time-domain SI methods. Conclusions and directions for future work are presented in Sec. VI.

II. Time-Domain SI Methods

A. Model Structures

Consider a continuous-time linear time-invariant (LTI) state-space model,

$$\dot{\boldsymbol{x}} = A\boldsymbol{x} + B\boldsymbol{u} + \boldsymbol{w} \tag{1a}$$

$$y = C\boldsymbol{x} + D\boldsymbol{u} + v \tag{1b}$$

where $\boldsymbol{u}$ is the input vector, y is the scalar output (multi-input/single-output case), $\boldsymbol{x}$ is the state vector and w and v are process and measurement noises, respectively. This model is completely defined by a state-space dimension n; the state-space matrices A, B, C, and D, and the noise covariances. The state-space dimension determines the dimensions of the state-space matrices. The identification problem is to determine the model order, the state-space matrices, and the noise covariances, so that the model output matches the observed data.

Many aeroelastic and flight dynamic behaviors result from changes in system dynamics brought about by changes in certain physical parameters. An example is aeromechanical instability in rotorcraft that occurs only at certain airspeeds and rotor speed. For such cases, a model of the form

$$\dot{\boldsymbol{x}} = A(\boldsymbol{\theta})\boldsymbol{x} + B(\boldsymbol{\theta})\boldsymbol{u} \tag{2a}$$

$$y = C(\boldsymbol{\theta})\boldsymbol{x} + D(\boldsymbol{\theta})\boldsymbol{u} \tag{2b}$$

where $\boldsymbol{\theta}$ is a time-varying (physical) parameter vector, is more reasonable than the LTI model (1). A system of this form is called a linear parameter-varying (LPV) system. It is a global model because it captures dynamics over a range of parameter values. The parameter vector typically consists of airspeed, angle of attack, rotor speed, etc. The system matrices are functions of the parameter–vector $\boldsymbol{\theta}$ and, during system operation, the parameter–vector changes with time. Thus, along each possible parameter trajectory, the system described by Eq. (2) is a linear time-varying system. Models of this form arise frequently in gain scheduling.

In many practical applications, natural frequencies and damping coefficients of the system may be known with some confidence, for example, $\omega_n \pm 0.2\omega_n$ for a 20% variation from the nominal natural frequency ω_n. When a priori information of this type is incorporated, the state-space matrix A becomes constrained or structured. For example, A may have the modal form

$$A = \operatorname{diag}\left\{ p_1, p_2, \ldots, p_{N_r}, \begin{bmatrix} 0 & 1 \\ -\omega_1^2 & -2\zeta_1\omega_1 \end{bmatrix}, \ldots, \begin{bmatrix} 0 & 1 \\ -\omega_{N_c}^2 & -2\zeta_{N_c}\omega_{N_c} \end{bmatrix} \right\} \tag{3}$$

where $\{p_k\}_{k=1}^{N_r}$ are the real poles and $\{(\omega_k, \zeta_k)\}_{k=1}^{N_c}$ are the poles with nonzero imaginary parts written in terms of natural frequency ω_k and damping coefficient ζ_k. It turns out that such structured SI problems are harder numerically than linear SI with no a priori information.

B. Subspace Algorithms for LTI Identification

A number of efficient techniques known as subspace identification methods have been developed to identify LTI models.[14–17] These techniques have some very nice theoretical properties and involve only matrix algebra. They reduce to the deterministic realization algorithm in the noise-free case and to the stochastic realization algorithm in the input-free ($u = 0$) case.[14–17]

Appendices A and B give a batch version of the basic subspace method and its recursive implementation, respectively. Step 2 of the batch subspace algorithm involves a singular value decomposition (SVD). It can be shown under certain conditions[15–17] that the number of nonzero singular values tend to the system order asymptotically. Thus, subspace methods can identify model orders from data. However, in practical applications where the number of samples is always finite, the model order r is usually fixed a priori. In this case, the algorithm in Appendix A gives a model of order at most r that best fits the data. A better strategy for model order determination is to modify the selection of principal components in step 3 using information-theoretic criteria such as those of Akaike, Bayes, and Rissanen (see Refs. 1, 2, and 9).

The online identification algorithm in Appendix B is based on two observations: 1) the least-squares problem can be solved recursively and 2) the quantity on the left-hand side of the SVD equation in step 2 of the batch algorithm is also a collection of Kalman states. As an illustration, consider an abruptly changing system of the form (1) where the state-space matrices are given by

$$A = \begin{bmatrix} 0 & 1 & 0 & 0 \\ -157.91 & -0.5 & 0 & 0 \\ 0 & 0 & 0 & 1 \\ 0 & 0 & -631.65 & -2.51 \end{bmatrix}, \qquad B = \begin{bmatrix} 0 \\ 1 \\ 0 \\ 1 \end{bmatrix}$$

$$C = \begin{bmatrix} 1 \\ 1 \\ 1 \\ 1 \end{bmatrix}^T, \qquad D = 0$$

for time $t \leq 20$ and

$$A = \begin{bmatrix} 0 & 1 & 0 & 0 & 0 & 0 \\ -157.91 & -0.5 & 0 & 0 & 0 & 0 \\ 0 & 0 & 0 & 1 & 0 & 0 \\ 0 & 0 & -631.65 & -2.51 & 0 & 0 \\ 0 & 0 & 0 & 0 & 0 & 1 \\ 0 & 0 & 0 & 0 & -1420 & -3.76 \end{bmatrix}$$

$$B = \begin{bmatrix} 0 \\ 1 \\ 0 \\ 1 \\ 0 \\ 1 \end{bmatrix}, \qquad C = \begin{bmatrix} 1 \\ 1 \\ 1 \\ 1 \\ 1 \\ 1 \end{bmatrix}^T, \qquad D = 0$$

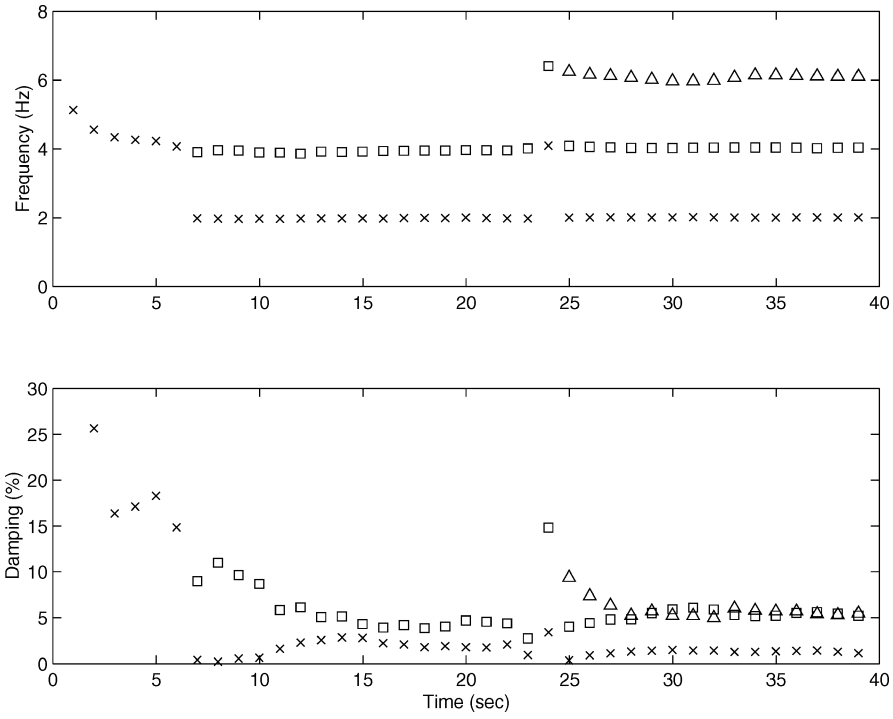

a)

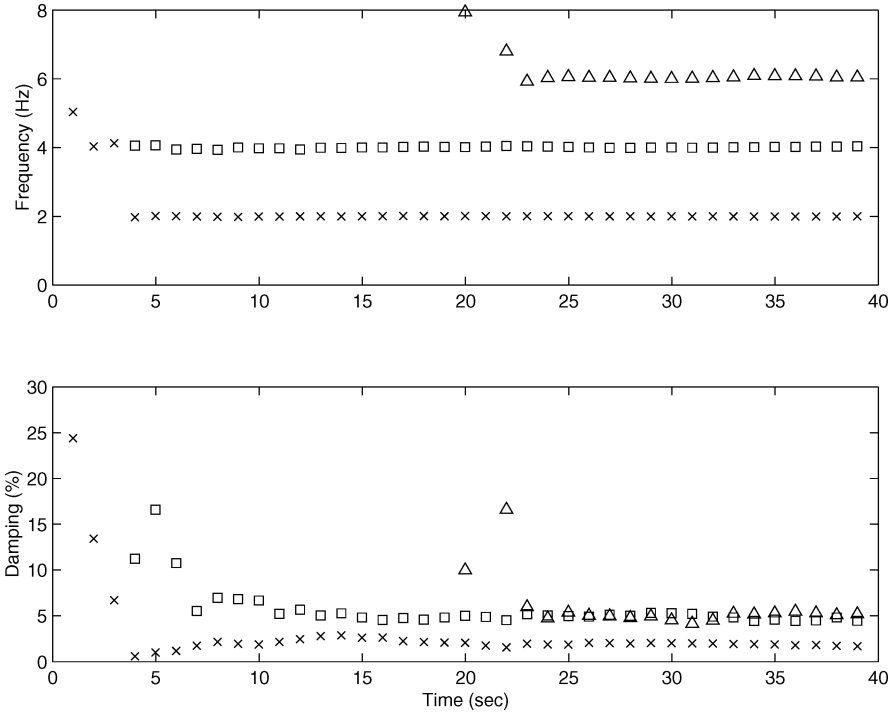

b)

Fig. 2 Identification of abrupt changes using online DSRA: a) $\lambda = 0.99$ and b) $\lambda = 0.95$.

for time $t > 20$. That is, the system has two modes with frequencies of 2 and 4 Hz until a third mode with frequency 6 Hz suddenly appears at time $t = 20$. We are interested in identifying and tracking all of the modes as they appear from input–output data.

Figure 2 shows the results of applying the online identification algorithm on simulated data with 5% additive noise at a sampling rate of 100 Hz. A wideband signal is used as input. If we use a model order that is equal to the true system order, then the algorithm will divide up the observed energy, part of which is due to noise, among the system modes leading to inaccurate estimates of natural frequencies and damping coefficients. Therefore, we must provide the algorithm with a conduit to bleed away some of the energy due to noise. To do this, we assume that (1) there are at most five modes instead of three and (2) all modes lie in the freqeuncy range [0, 10] Hz. The upper bound on the number of modes is also used to determine the size of recursive least-squares problem, whereas the bound on the frequency range is used to truncate spurious modes from the identified model. Figures 2a and 2b correspond to identification with forgetting factor $\lambda = 0.99$ and $\lambda = 0.95$, respectively. The forgetting factor $0 < \lambda \leq 1$ (algorithm in Appendix B) assigns the weight λ^k for data that were obtained k time steps ago. Thus, with large values of λ, the influence of past data lingers longer and slows

down identification of new modes. On the other hand, with small values of λ, the information in past data is disregarded in favor of new data, causing faster identification of new modes. With $\lambda = 0.99$, approximately 200 samples (2 s) are needed to bring the effect of past data to about 10%. The same reduction requires approximately 40 samples when $\lambda = 0.95$.

In Fig. 2, the algorithm begins tracking a single mode, which eventually converges to the 4-Hz mode, although the system has two modes (2 and 4 Hz). This is because lower frequency modes generally require more time to identify. When $\lambda = 0.99$, the algorithm identifies both 2- and 4-Hz modes by about 6 (12 cycles of 2-Hz mode) from the noisy data. There is a 2-s improvement with $\lambda = 0.95$, as shown in Fig. 2b. To explain the slower convergence in the damping coefficients, consider the second-order transfer function

$$g(s) = 1 \Big/ \left(s^2 + 2\zeta\omega_n s + \omega_n^2\right)$$

and its sensitivity to the damping coefficient ζ and natural frequency ω_n,

$$\mathrm{d}g(s) = -2g(s)^2[(\zeta s + \omega_n)\,\mathrm{d}\omega_n + \omega_n s\,\mathrm{d}\zeta]$$

$$= -2\omega_n g(s)^2\left[(\zeta s + \omega_n)\frac{\mathrm{d}\omega_n}{\omega_n} + \zeta s\frac{\mathrm{d}\zeta}{\zeta}\right]$$

We see from the second equality that the transfer function is less sensitive to changes in damping coefficient than to changes in natural frequency. As a result, when damping coefficient and natural frequencies are to be identified simultaneously, we can expect slower convergence and a greater percentage error in damping estimate than in natural frequency estimate.

The remarkable aspect of this numerical experiment is the identification and tracking of the 6-Hz mode, which appears in the real system at $t = 20$, without losing track of the other modes. There is a 4-s delay in identifying the new mode when $\lambda = 0.99$, which is partly due to noise in the data and partly due to the effect of past data as explained. There is virtually no delay in detecting the change when $\lambda = 0.95$. In Fig. 2a, the algorithm seems to have lost track of the 2-Hz mode momentarily at about 24 s. This is not a generic behavior, and we have not observed it in other runs.

This example is meant to show that there are time-domain algorithms that can be used to identify and track structural modes. Obviously, these algorithms have certain limitations in their present form. A comprehensive study of such algorithms is required. We shall touch on this issue in Sec. V.

III. V-22 Structural Mode Identification

Controller design for systems with both rigid-body and structural dynamics is usually carried out in two steps. First, a feedback controller is designed using only the rigid-body model. Structural modes are then taken care of by inserting appropriate notch filters in the feedback path to remove those structural modes that may destabilize the system. In some cases, notch filters are placed in the forward path as well, to avoid spurious feedback through the system's actuators. The notch filter's center frequency is tuned to the natural frequency of the corresponding structural mode. However, the structural mode frequency changes with gross weight, sling loads, and airspeed. Therefore, a notch filter that is designed for certain flight conditions may become ineffective for other conditions. To account for these variations, notch filters must be designed wider than required so that they remain effective within the entire range of possible structural mode frequencies. However, as phase lag increases with notch width, the notch filters introduce undesirable lag into the system, causing degradation in overall performance and possibly instability.[18]

Another approach is to estimate the structural mode frequencies in flight and use them as center frequencies. This approach requires a reliable time-domain SI method that can rapidly estimate multiple modal frequencies from MIMO data online. As a first step toward the development of an online structural mode tracking algorithm, we evaluated a batch subspace method called the deterministic–stochastic realization algorithm (DSRA) on V-22 engineering and manufacturing development flight-test data. The standard industrial practice for verifying damping of V-22 structural modes is to excite each individual mode with a sine dwell and calculate the damping coefficient from the decay using the modified Prony curve fit method (see Refs. 19 and 20). The modified Prony method is less sensitive to noise and has been validated extensively for use in V-22 ground- and flight-test data analysis. It is the baseline method against which the performance of DSRA will be compared for the critical antisymmetric wing chord, symmetric wing beam (SWB), symmetric wing chord, and symmetric wing torsion modes.[18] We will also show that the batch DSRA method can identify multiple modes from a single sine sweep excitation, which cannot be done with the Prony method. This represents great savings on flight-test time, particularly during high-speed dive maneuvers, which are very demanding on the pilot.

Table 1 Comparison of modified Prony method and batch DSRA for SWB mode identification

	Sine dwell		Sine sweep	
Mode	$\omega(\sigma_\omega)$, Hz	$\zeta(\sigma_\zeta)$, %	$\omega(\sigma_\omega)$, Hz	$\zeta(\sigma_\zeta)$, %
SWB 150 kn				
Prony (from SWB)	2.89 (0.05)	2.10 (0.29)	N/A	N/A
DSRA (from SWB)	2.87 (0.01)	1.93 (0.21)	2.83 (∗)	2.86 (∗)
DSRA (from acceleration)	2.88 (∗)	1.87 (∗)		
SWB 200 kn				
Prony (from SWB)	2.86 (0.02)	3.2 (0.32)	N/A	N/A
DSRA (from SWB)	2.82 (0.02)	3.0 (0.31)		
SWB 250 kn				
Prony (from SWB)	2.82 (0.05)	3.6 (0.5)	N/A	N/A
DSRA (from SWB)	2.82 (0.03)	3.7 (0.5)		
SWT 150 kn				
Prony			N/A	N/A
DSRA			5.18	4.58

A summary of the quantitative results for SWB mode is given in Table 1. In Table 1, ω, ζ, and σ_ω and σ_ζ are natural frequency, damping coefficient, and their empirical standard deviations, and an asterisk denotes not computed. The natural frequency and damping coefficient estimates from Prony and DSRA compare very well. The larger standard deviations in damping coefficient are to be expected in view of our earlier comments regarding transfer function sensitivity. Table 1 also shows results of applying batch DSRA to sine sweep data. The estimates of frequencies and damping coefficients for multiple modes obtained by DSRA from a single sine sweep agree very well with the estimates from sine dwells. Similar results are presented for the SWC sine dwell excitation in Fig. 3. Based on these and other comparisons[18] of the DSRA method with Prony, the following conclusions can be drawn: 1) Natural frequencies and damping coefficients estimated by batch DSRA from sine dwells and sine sweeps are in good agreement with the corresponding Prony estimates from sine dwells, 2) Sine sweeps and other inputs can be used to estimate more than one mode simultaneously using DSRA, and 3) DSRA and Prony are both sensitive to signal to noise ratio (SNR), which relates to fundamental issues of identifiability. The design of proper input signals to improve SNR is an important topic.[1–3,6]

IV. Identification of Models of Aeromechanical Instability

Active control of rotorcraft aeromechanical instability such as ground resonance involves designing controllers that provide stability over a wide range of operating conditions, subject to safety constraints on system response and saturation constraints on actuator inputs. The key difficulty in applying control techniques is the lack of state-space models of the physical phenomenon near and beyond the instability boundaries. Because we cannot conduct open-loop experiments for SI near and beyond the instability boundaries, the following procedure is required.

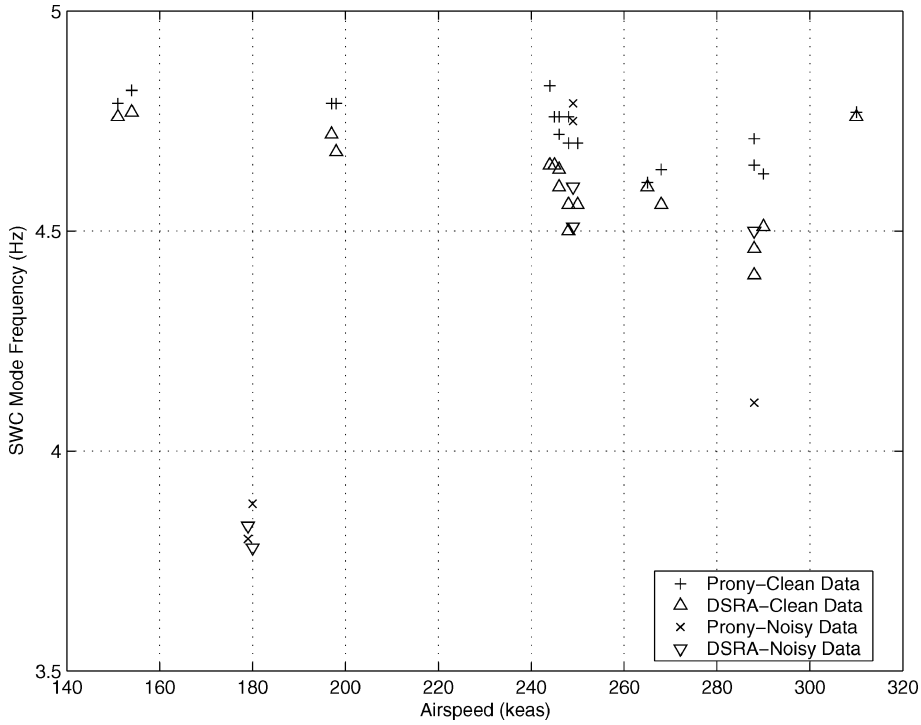

a)

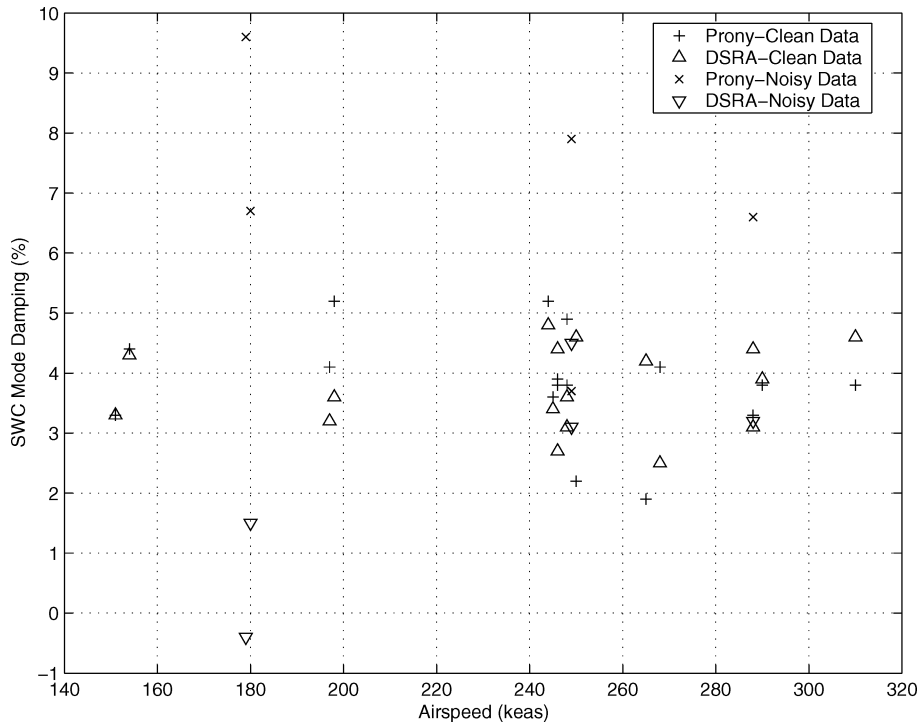

b)

Fig. 3 Comparison of Prony and batch DSRA estimates for a) SWC frequency and b) damping coefficient.

1) Begin at a known stable operating point. In the ground resonance problem, the operating point is defined by a single variable, rotor speed. Conduct an open-loop experiment for SI at this stable operating point, for example, $\boldsymbol{\theta}_0$.

2) Identify a state-space model valid locally (in the neighborhood of the operating point) from the experimental data using the methods described. Design a controller that guarantees robust stability using $\mathcal{H}_\infty$ techniques using the identified model.

3) Close loop with the controller from the preceding step, move a bit toward the instability boundary, for example, increase rotor speed from $\boldsymbol{\theta}_0$ to $\boldsymbol{\theta}_1$ within the stability region of the controller in the ground resonance problem. Conduct a closed-loop experiment for SI at the new operating point $\boldsymbol{\theta}_1$.

4) Repeat steps 2 and 3 until the desired operating envelope is covered.

Note that, at each operating point $\boldsymbol{\theta}_k$, we identify a linear model of the open-loop plant of the form (1) where the state-space matrices should be subscripted with the letter k to emphasize validity at $\boldsymbol{\theta}_k$. The collection of models $\{(\theta_k, A_k, B_k, C_k, D_k)\}_{k=0}^{N}$ can be used to describe the aeromechanical phenomenon over the entire operational range via the LPV state-space model (2) where the time-varying parameter is the operating condition variable $\boldsymbol{\theta}$. In the

ground resonance problem with a scalar variable defining operating point, we have

$$A(\theta) = \begin{cases} A_i & \text{if} \quad \theta = \theta_i \\ \beta A_i + (1-\beta)\, A_{i+1} & \text{if} \quad \theta_i < \theta < \theta_{i+1} \end{cases}$$

where

$$\beta = (\theta_{i+1} - \theta)/(\theta_{i+1} - \theta_i)$$

Similar expressions hold for the remaining state-space matrices. Details of this approach and its experimental validation on the cobra stick model (CSM) facility at Bell Helicopter Textron, Inc. can be found in Ref. 21. Here, we summarize the identification results.

Figure 4 shows locations of test inputs and acceleration measurements taken for identification. Figure 4b shows 5 the stability behavior of CSM. The CSM is unstable at approximately 36 Hz and technically stable elsewhere. However, because of the large vibratory amplitudes, open-loop experiments are not feasible in the rotor speed range 34–37 Hz. (These numbers are not representative of any rotorcraft.)

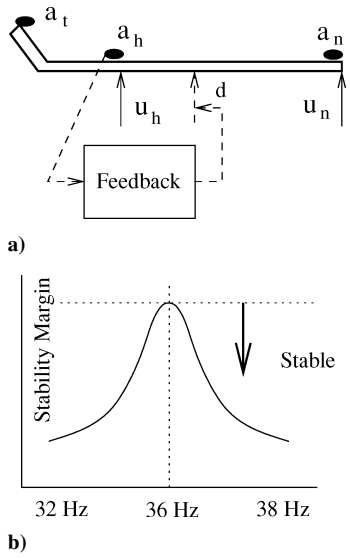

Fig. 4 Schematic of CSM experimental setup.

The identification procedure began with an open-loop experiment at 32 Hz. The input–output data collected are shown in Fig 5. The test inputs are wideband noises intended to excite all of the structural modes. The state-space model identified by DSRA from these data in modal coordinates is

$$\dot{\boldsymbol{x}} = \begin{bmatrix} 0 & -1.0 & 0 & 0 & 0 & 0 \\ 2.1 \times 10^4 & -0.9 & 0 & 0 & 0 & 0 \\ 0 & 0 & 0 & -1.0 & 0 & 0 \\ 0 & 0 & 4.0 \times 10^4 & 0 & 0 & 0 \\ 0 & 0 & 0 & 0 & 0 & -1.0 \\ 0 & 0 & 0 & 0 & 5.3 \times 10^4 & -2.5 \end{bmatrix} \boldsymbol{x} + \begin{bmatrix} 0 & 0 \\ -2.6 & -2.9 \\ 0 & 0 \\ 0 & -0.3 \\ 0 & 0 \\ -2.1 & -9.5 \end{bmatrix} \boldsymbol{u}$$

$$y = \begin{bmatrix} -342.2 & 4.6 & 670.9 & 1.3 & 655.3 & -1.5 \\ -23.3 & 0.1 & -57.3 & -1.0 & -482.7 & 1.0 \end{bmatrix} \boldsymbol{x} + \begin{bmatrix} -0.04 & -0.04 \\ -0.04 & 0.02 \end{bmatrix} \boldsymbol{u}$$

whose natural frequencies are 23, 32, and 36.8 Hz. The associated damping coefficients are 0.34, 0 and 0.5%. The estimated mode at 32 Hz appears to be neutrally stable, but in fact it is a lightly damped mode. This is also the mode that varies with rotor speed. An $\mathcal{H}_\infty$ controller was designed using the identified model and a closed-loop experiment was performed at 33 Hz. The procedure was continued until the whole rotor speed range was covered.

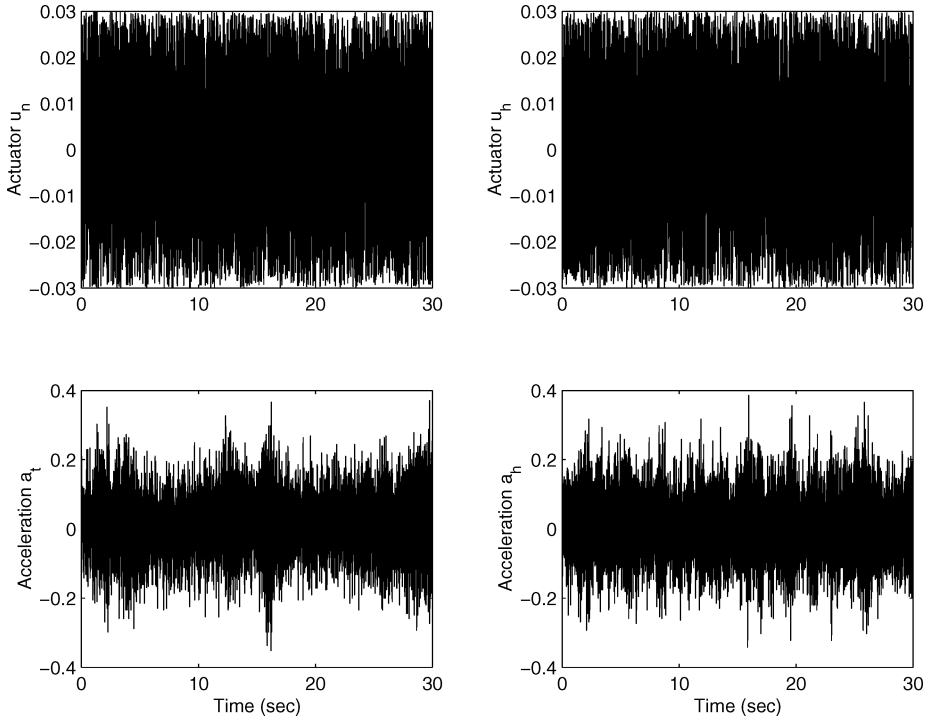

Fig. 5 Input–output data from open-loop experiment at 32 Hz on CSM.

Table 2 Modes estimated using DSRA from open- and closed-loop experiments

Experiment	Mode 1	Mode 2	Mode 3
32 Hz, open loop	23 Hz, 0.34%	32 Hz, 0%	36.8 Hz, 0.5%
33 Hz, closed loop	23.071 Hz, 0.5%	33.014 Hz, 0.12%	37.263 Hz, 1.09%
33 Hz, open loop	23.073 Hz, 0.34%	33.017 Hz, 0%	36.818 Hz, 0.29%
34 Hz, closed loop	23.06 Hz, 0.34%	34.00 Hz, 0.1%	36.81 Hz, 0.2%
36 Hz, closed loop	23.131 Hz, 1.08%	36.21 Hz, 0.28%	
38 Hz, closed loop	23.06 Hz, 0.32%	36.86 Hz, 0.05%	37.99 Hz, 0.2%

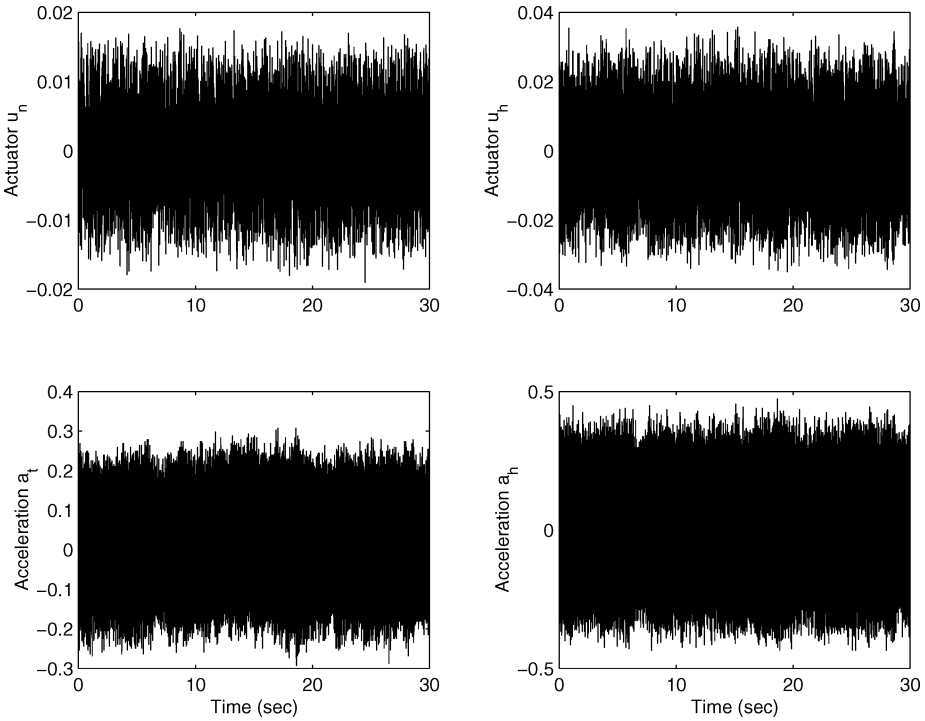

Fig. 6 Input–output data from closed-loop experiment at 36 Hz on CSM.

Table 2 shows the natural frequencies and damping coefficients estimated using the iterative controller design and closed-loop experiment procedure. Results from open- and closed-loop data at 33 Hz are provided for the purposes of comparison. The frequencies and damping coefficients agree very well, indicating that the subspace method can be used to identify open-loop structural modes from closed-loop experimental data, provided that the controller is known. Prony's method and frequency-domain identification methods cannot accurately compute open-loop structural modes from closed-loop data due to the mode changes introduced by control and due to the possibility of pole-zero cancellations, whereas certain time-domain methods produce bias errors in frequency and damping estimates due to the feedback loop.[22] Figure 6 shows closed-loop experimental data at 36 Hz. To conduct this experiment, we used a linear controller designed from the identified model at 35 Hz that provided enough stability margin. In this model development effort that combines identification and controller design, the main issue is the reliability of identified models. Our experimental results suggest that subspace methods can provide the measure of reliability needed for SI of unstable phenomenon.

V. Further Research and Development

The area of time-domain SI has seen tremendous growth in the past two decades. The subspace algorithms have found applications in other fields, including process control. There are other algorithms, most notably for nonlinear SI, that may be successful in flight vehicle modeling and analysis. A comprehensive study to classify identification problems arising in flight dynamics and to compare various algorithms for their solution is long overdue. In addition, the following three areas are suggested for further research and development.

A. Experiment Design

The reliability of any model identified from experimental data is dependent to a great extent on the experiment itself. The conventional 3–2–1–1, doublet and sine dwell inputs are not necessarily the best inputs for linear SI and, in particular, structural mode identification. The problem of input design, also known as experiment design, has been the subject of vigorous research. At present, experiment design for linear SI is completely solved, and there is a general framework for addressing constrained and nonlinear systems. However, experiment design for high-angle-of-attack flight dynamics and unstable flight regimes have not received the same level of attention. The use of experiment design methods in industry can reduce the amount of testing and improve safety.

B. Estimation of Uncertainty

There are essentially three sources of uncertainties in an identified model. The first source is unmodeled dynamics, that is, the gap between system dynamics and model dynamics. This nonparametric uncertainty is well known in control systems, but rarely mentioned in identification literature. The second source is noise in the data used for model identification, which causes parameters of the model to be uncertain. Parametric uncertainty can be deterministic, for example, $p \in [p_{\min}, p_{\max}]$, or stochastic, for example, p is a Gaussian with mean $\bar{p}$ and variance σ. The third source of uncertainty deals with the amount of discriminatory information contained in the data that permits the identification of individual parameters. It is related to experiment design and identifiability of the model set. Computation of modeling uncertainties from data is a difficult problem, and very little, if any thing is known about it. The MLE technique may be able to determine parametric

uncertainties. A deeper look into this issue is suggested for future work.

C. Online Structural Mode Tracking

Structural modes of an aircraft may change slowly due to flight condition changes and abruptly due to failure and damage. These changes degrade performance and can even be catastrophic unless estimated rapidly and compensated for. A recursive subspace algorithm with the capability to track structural modes is presented in this paper. However, many issues remain to be studied, including sensitivity to noise and test inputs. A focused effort to develop and validate online identification algorithms is needed.

VI. Conclusions

Subspace algorithms are time-domain SI methods for MIMO systems. They use linear algebraic operations only and can be implemented for batch and online data processing. We evaluated these algorithms using two prototypical aircraft applications. The application to V-22 structural mode identification is prompted by a need for online modal frequency estimation stemming from notch filter implementation, as well as a need to reduce the cost of ground and flight testing. Our results show that subspace methods compare very well with the traditional Prony method in sine dwell experiments. We also showed that multiple structural modes can be identified from a single sine sweep experiment, which is not possible with the Prony method. The application to aeromechanical instability is interesting on several counts, including the infeasibility of open-loop experimentation. Our results show that subspace methods can be used in an iterative closed-loop experimentation and controller design strategy to identify models of parameter-dependent unstable phenomena. The identification of open-loop unstable modes from closed-loop data is difficult with Prony and frequency-domain methods.

Appendix A: Batch Version of a Subspace Algorithm

The basic subspace algorithm that follows may be found in various forms in Refs. 14–17. Given a sequence of vectors $\{y_k\}_{k=1}^{N}$, the $Y_{i|l}$ is the Hankel matrix,

$$Y_{i|l} = \begin{bmatrix} y_i & y_{i+1} & \cdot & \cdot & \cdot & y_{i+j-1} \\ y_{i+1} & y_{i+2} & \cdot & \cdot & \cdot & y_{i+j} \\ \cdot & \cdot & \cdot & \cdot & \cdot & \cdot \\ \cdot & \cdot & \cdot & \cdot & \cdot & \cdot \\ y_l & y_{l+1} & \cdot & \cdot & \cdot & y_{l+j-1} \end{bmatrix} \tag{A1}$$

where i, j, and l are given positive integers.

Let $r > 0$ be a specified model order. Fix integers i and j such that $r < i < j$ and $N = 2i + j - 1$. The following steps compute a state-space realization of order r:

1) Solve the least-squares problem for L_p and T_d,

$$\min_{L_p, T_d} \left\| Y_{i+1|2i} - L_p \begin{bmatrix} U_{1|i} \\ Y_{1|i} \end{bmatrix} - T_d U_{i+1|2i} \right\|_F \tag{A2}$$

where $U_{1|i}$, $Y_{1|i}$, $U_{i+1|2i}$ and $Y_{i+1|2i}$ are matrices constructed from the data as shown in Eq. (A1).

2) Perform the SVD

$$L_p \begin{bmatrix} U_{1|i} \\ Y_{1|i} \end{bmatrix} = U \Sigma V'$$

where the diagonal elements of Σ are ordered from the largest to the smallest.

3) Partition U, Σ, and V as follows:

$$U = \begin{bmatrix} U_1 & U_2 \end{bmatrix}, \qquad \Sigma = \begin{bmatrix} \Sigma_1 & 0 \\ 0 & \Sigma_2 \end{bmatrix}, \qquad V = \begin{bmatrix} V_1 & V_2 \end{bmatrix}$$

where U_1 and V_1 have r columns and Σ_1 contains the largest r singular values.

4) Compute the Kalman states as follows:

$$\hat{X}_{i+1|i+1} = [\hat{\boldsymbol{x}}_{i+1} \quad \hat{\boldsymbol{x}}_{i+2} \quad \cdot \quad \cdot \quad \cdot \quad \hat{\boldsymbol{x}}_{i+j}] = \Sigma_1^{\frac{1}{2}} V_1' \tag{A3}$$

5) Solve the least-squares problem,

$$\min_{A_d, B_d, C_d, D_d} \left\| \begin{bmatrix} \hat{\boldsymbol{x}}_{i+2} & \cdot & \cdot & \hat{\boldsymbol{x}}_{i+j} \\ y_{i+1} & \cdot & \cdot & y_{i+j-1} \end{bmatrix} - \begin{bmatrix} A_d & B_d \\ C_d & D_d \end{bmatrix} \begin{bmatrix} \hat{\boldsymbol{x}}_{i+1} & \cdot & \cdot & \hat{\boldsymbol{x}}_{i+j-1} \\ \boldsymbol{u}_{i+1} & \cdot & \cdot & \boldsymbol{u}_{i+j-1} \end{bmatrix} \right\|_F \tag{A4}$$

to obtain a discrete-time model. Noise covariances are obtained from the residual error.

6) Convert to continuous-time to get state-space model.

Step 2, which involves the SVD of a large matrix, is the most computationally demanding part of the algorithm. This step is used to determine the principal directions that are to be retained when computing a fixed-order model. The SVD is usually replaced with a quadratic regulator QR factorization. In most implementations of the subspace algorithm, steps 4 and 5 are also replaced with algebraic computations that are less intensive.

Appendix B: Online Version of a Subspace Algorithm

An online version of the basic subspace algorithm is described next. For convenience, the recursive least-squares algorithm[2] is denoted by RLS($\cdot$). The forgetting factor $0 < \lambda \leq 1$ in the implementation given next is used to weight immediate past more and distant past exponentially less. It is useful in estimating system models for time-varying systems.

Suppose that $\{u_k,\ y_k\}_{k=1}^{N}$ is given. Fix integers i and j such that $i < j$ and $N = 2i + j - 1$. Fix $0 < \lambda \leq 1$. The following steps give a recursive implementation of the basic subspace method.

Initialization: Choose initial values for the matrix L_p, the states, the state-space realization, and their covariances:

$$L_p^0, \qquad x_0, \qquad G_0 = \begin{bmatrix} A_{d0} & B_{d0} \\ C_{d0} & D_{d0} \end{bmatrix}, \qquad G_c^0 > 0, \qquad L_c^0 > 0$$

Recursive loop: for $k = 1, 2, \ldots,$ is next.

Define column vectors:

$$P = [\boldsymbol{u}'_{j+k} \quad \cdots \quad \boldsymbol{u}'_{i+j+k-1} \quad y'_{j+k} \quad \cdots \quad y'_{i+j+k-1}]'$$

$$U_f = [\boldsymbol{u}'_{i+j+k} \quad \cdots \quad \boldsymbol{u}'_{2i+j+k-1}]'$$

$$Y_f = [y'_{i+j+k} \quad \cdots \quad y'_{2i+j+k-1}]'$$

Update L_p:

$$\left[L_p^k, L_c^k\right] = \text{RLS}\left(L_p^{k-1},\ L_c^{k-1},\ \begin{bmatrix} P \\ U_f \end{bmatrix},\ Y_f,\ \lambda\right)$$

Update x:

$$x_k = L_p^k P$$

Update G:

$$\left[G_k, G_c^k\right] = \text{RLS}\left(G_{k-1},\ G_c^{k-1},\ \begin{bmatrix} x_{k-1} \\ u_{i+j+k-1} \end{bmatrix}, \begin{bmatrix} x_k \\ y_{i+j+k-1} \end{bmatrix}, \lambda\right)$$

The state-space model G_k is the updated discrete-time model, and G_c^k is its covariance. As in the batch algorithm, some of the preceding steps can be improved. For example, we can determine a state-space model directly from L_p^k by performing an SVD. This model is more accurate than the RLS-updated model given by the preceding algorithm due to the slower convergence of RLS. However, SVD is computationally more intensive than RLS. The SVD approach is

appropriate for applications in which the state-space model needs updating at a slower rate than the rate at which data are sampled, for example, slowly time-varying system.

Acknowledgments

The work presented in Secs. III and IV was done jointly with Bell Helicopter Textron, Inc., under funding from the U.S. Navy [Naval Air Warfare Center (NAWC) Aircraft Division] and NASA Ames Research Center. We wish to thank Richard Bennett, Thomas Parham, and Ross Brown of Bell Helicopter for their support. We also wish to thank Marc Steinberg (NAWC) and Stephen Jacklin (NASA Ames), who served as Technical Monitors, for their support and encouragement.

References

[1]Goodwin, G., and Payne, R., *Dynamic System Identification: Experiment Design and Data Analysis*, Academic Press, New York, 1977.

[2]Ljung, L., *System Identification: Theory for the User*, 2 ed., Prentice–Hall, New York, 1999.

[3]Mehra, R., and Lainiotis, D., *System Identification: Advances and Case Studies*, Academic Press, New York, 1976.

[4]Gupta, N., and Mehra, R., "Computational Aspects of Maximum Likelihood Estimation and Reduction in Sensitivity Function Calculations," *IEEE Transactions on Automatic Control*, Vol. 19, No. 6, 1974, pp. 774–783.

[5]Dempster, A., Laird, N., and Rubin, D., "Maximum Likelihood from Incomplete Data via the EM Algorithm," *Journal of the Royal Statistical Society*, Ser. B, Vol. 39, No. 1, 1977, pp. 1–38.

[6]Mehra, R., "Optimal Input Signals for Parameter Estimation in Dynamic System: Survey and New Results," *IEEE Transactions on Automatic Control*, Vol. 19, No. 6, 1974, pp. 753–768.

[7]Hamel, P., and Jategaonkar, R., "Evolution of Flight Vehicle System Identification," *Journal of Aircraft*, Vol. 33, No. 1, 1996, pp. 9–28.

[8]Hamel, P., and Jategaonkar, R., "The Role of System Identification for Flight Vehicle Applications—Revisited," *Proceedings of System Identification for Integrated Aircraft Development and Flight Testing*, Research and Technology Organization, Neuilly-Sur-Seine Cedex, France, March 1999; also Paper No. 2.

[9]Klein, V., and Morelli, E., *System Identification Applied to Aircraft—Theory and Practice*, AIAA, Reston, VA, 2001.

[10]Padfield, G. D. (ed.), "Application of System Identification in Rotorcraft Flight Dynamics," *Vertica,* special ed. Vol. 13, No. 3, 1989.

[11]Tischler, M., "Frequency-Response Identification of XV-15 Tilt-Rotor Aircraft Dynamics," NASA TM-89428, May 1987.

[12]Tischler, M., "System Identification Methods for Aircraft Flight Control Development and Validation," NASA Ames Research Center, NASA TM-110369, Oct. 1995.

[13]Morelli, E., "In-Flight System Identification," AIAA Paper 98-4261, Aug. 1998.

[14]Mehra, R., "Identification of State Space Models Using a Stochastic Realization Algorithm with Applications to Modal Identification of Flexible Aerospace Structures," *Proceedings of the 9th IFAC/IFORS Symposium on Identification and System Parameter Estimation*, Pergamon, Oxford, England, UK, July 1991.

[15]Van Overschee, P., and De Moor, B., *Subspace Identification for Linear Systems*, Kluwer, Dordrecht, The Netherlands, 1996.

[16]Verhaegen, M., "Identification of the Deterministic Part of MIMO State Space Models Given in Innovations Form From Input–Output Data," *Automatica*, Vol. 30, No. 1, 1994, pp. 61–74.

[17]Viberg, M., "Subspace-Based Methods for the Identification of Linear Time-Invariant Systems," *Automatica*, Vol. 31, No. 12, 1995, pp. 1835–1851.

[18]Mehra, R., Nagpal, K., Parham, T., and Bennett, R., "Self-Adaptive Notch Filter for the V-22 Flight Controls Using Stochastic Realization Algorithm (SRA)" Scientific Systems Co., Final Rept. Contract N62269-96-C-0030, Woburn, MA, April 1998.

[19]Braun, S., and Ram, Y., "Determination of Structural Modes via the Prony Method: System Order and Noise Induced Poles," *Journal of the Acoustical Society of America*, Vol. 81, No. 5, 1987, pp. 1447–1459.

[20]Osborne, M., and Smyth, G., "A Modified Prony Algorithm for Exponential Function Fitting," *SIAM Journal on Scientific Computing*, Vol. 16, No. 1, 1995, pp. 119–138.

[21]Prasanth, R., Mehra, R., Bennett, R., and Brown, R., "Active Control of Aeromechanical Instability—Identification, Controller Design and Experimental Results," *Proceedings of the American Helicopter Society National Specialists' Meeting*, Bridgeport, CT, Oct. 2000.

[22]Forssell, U., and Ljung, L., "Issues in Closed Loop Identification," Linkoping Univ., Rept. LiTH-ISY-R-1940, Linkoping, Sweden, April 1997.